Perfect Surface Wave Cloaks

R. C. Mitchell-Thomas,[1] T. M. McManus,[1] O. Quevedo-Teruel,[1] S. A. R. Horsley,[2] and Y. Hao[1,*]

[1]School of Electronic Engineering and Computer Science, Queen Mary University of London, London E1 4NS, United Kingdom
[2]Department of Physics and Astronomy, University of Exeter, Exeter EX4 4QL, United Kingdom

(Received 11 September 2013; published 19 November 2013)

This Letter presents a method for making an uneven surface behave as a flat surface. This allows an object to be concealed (cloaked) under an uneven portion of the surface, without disturbing the wave propagation on the surface. The cloaks proposed in this Letter achieve perfect cloaking that only relies upon isotropic radially dependent refractive index profiles, contrary to those previously published. In addition, these cloaks are very thin, just a fraction of a wavelength in thickness, yet can conceal electrically large objects. While this paper focuses on cloaking electromagnetic surface waves, the theory is also valid for other types of surface waves. The performance of these cloaks is simulated using dielectric filled waveguide geometries, and the curvature of the surface is shown to be rendered invisible, hiding any object positioned underneath. Finally, a transformation of the required dielectric slab permittivity was performed for surface wave propagation, demonstrating the practical applicability of this technique.

DOI: 10.1103/PhysRevLett.111.213901 PACS numbers: 41.20.−q, 42.15.−i, 73.20.Mf

Cloaking free-space waves, using a combination of metamaterials and the theory of transformation optics, has been the focus of much attention since the idea was proposed in 2006 [1,2]. While the advances that have been made show much promise for this goal, many limitations have been demonstrated that restrict the performance of such devices. For example, highly dispersive materials are required in order to obtain superluminal phase velocities. The function of such devices is thus inherently narrow band [3]. Also, the losses associated with the metamaterials required, produce shadowing [4], and the anisotropy requirements create the need for highly complex structures to implement the cloaks [5].

More recently, designs for cloaking devices applied to surface waves have been investigated [6–12], which can be divided into two groups. The first is a version of Pendry's cloak design [1], appropriate for surface wave propagation. However, this cloak also requires anisotropy, where some of the axial components of the permittivity and permeability tensors are not only below unity, but reach zero [6–8]. This implies a surface that would excite leaky waves, producing radiation losses [13], demonstrating that these cloaks are necessarily imperfect.

The second set of surface wave cloak designs is an appropriate implementation of the carpet cloak idea [6,7,9,10], but the drawback here is that the cloaks are large compared to the wavelength, necessarily larger than the cloaked object, and include approximations limiting the accuracy of the cloak. In addition, some of these designs for surface wave cloaks have the disadvantage of being unidirectional [10], which limits the use in a practical application.

This Letter presents a solution to surface wave cloaking, where an object can be hidden underneath a bump in a surface. It is achieved by utilizing curved geometries combined with graded index media to create perfect, isotropic, omnidirectional cloaks which can be used to make the curvature of a surface appear invisible. This is a general theory that can be utilized for the design of cloaks for numerous surface wave phenomena, such as linear surface waves in fluid [14] or bending modes in thin elastic plates [15], but here it is electromagnetic surface wave cloaks that are investigated. These cloaks could be applied to the design of conformal surface wave-based [16] antenna devices [17,18] which are retrofitted to vehicles or airborne platforms, where perturbations of the surface are necessary for structural or aerodynamic reasons, but create scattering of the surface waves which is detrimental to their performance.

Suppose we have a rotationally symmetric curved surface on which waves can propagate. A layer of material with a given refractive index placed above the surface will modify the effective distance seen by these waves. This index profile will ensure the propagation characteristics of a flat plane are emulated by the curved one, thus making the curvature invisible to waves confined to this surface. It can be derived using the same technique that was used to determine the Maxwell-fish eye profile from a sphere [19,20], but in the converse sense. Rather than utilizing a graded index on a flat plane that emulates the ray behavior on a sphere, here it is the ray behavior on a flat homogeneous plane that is being reproduced by a curved surface with a graded index. The latter is calculated by equating the optical path length of a ray as it traverses across a flat plane with homogeneous refractive index, to the optical path on the rotationally symmetric curved surface with a refractive index that depends on the angle, for two orthogonal paths. The first is a circular path (of fixed radius), illustrated in Fig. 1 in red. The second is a radial path (of fixed angle) which connects the outer radius of the device, $r = a$, to the central point, $r = 0$, shown in blue in Fig. 1.

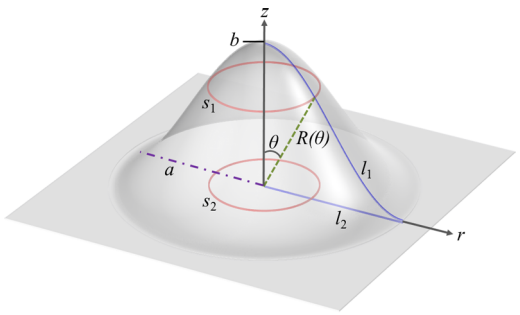

FIG. 1 (color online). A diagram illustrating the orthogonal ray paths that are equated in order to derive the appropriate index distribution to cloak a particular surface, of radius a and height b. The blue lines are the radial geometric path lengths (l_1 and l_2) and the red lines denote the circular geometric paths (s_1 and s_2), in the curved space and flat space. The green dashed line denotes the length from the origin to the surface, $R(\theta)$.

The infinitesimal optical path elements of a ray traversing the two radial geometric paths, l_1 and l_2, are equated to give

$$n(\theta)\sqrt{R(\theta)^2 + R'(\theta)^2}d\theta = dr \tag{1}$$

and the optical path length of a ray following the two circular geometric paths, s_1 and s_2, are equated to give

$$2\pi R(\theta)\sin(\theta)n(\theta) = 2\pi r. \tag{2}$$

Equations (1) and (2) can then be combined, and after some manipulation, take the form

$$\frac{n'(\theta)}{n(\theta)} = \frac{\sqrt{R(\theta)^2 + R'(\theta)^2} - R'(\theta)\sin(\theta) - R(\theta)\cos(\theta)}{R(\theta)\sin(\theta).} \tag{3}$$

This general approach can be applied to any rotationally symmetric surface deformation, provided that the slope of the surface dz/dr does not change sign. Three surface cloaks are demonstrated in this Letter. The first case study is the antifish eye cloak, so named because while the Maxwell-fish eye lens is the mapping of a hemisphere onto a flat plane, this index distribution is calculated with a mapping of a flat plane onto a hemisphere. This is a relatively simple distribution to derive, since the radius of the surface does not depend on the angle. The analytical solution to Eq. (3) is $n(\theta) = \tan(\theta/2)/\sin(\theta)$, and is valid for any radius a of the hemispherical surface. Although the index distribution here perfectly corrects the phase difference of the waves traversing the sphere, to equal those that only propagate across the flat plane, this system will produce reflections at the boundary of the surface due to the 90° transition between the flat and the spherical surfaces. For this reason, the second design was chosen to have a conical shape, and this also has an analytical solution of the form $n(\theta) = a\gamma/(\int_0^{(\pi/2)}(\gamma\beta/R(\theta)\sin(\theta))d\theta)R(\theta)\sin(\theta)$, where $\beta = \sqrt{R(\theta)^2 + R'(\theta)^2}$ and $\gamma = \exp(\int(\beta/R(\theta)\sin(\theta))d\theta)$, valid when $b < a$. This index distribution reaches asymptotically to zero at $r = 0$, but to a good approximation, this can be truncated to a quarter of the maximum. While the conical cloak reduces the reflections from the boundary, it does not remove them completely, particularly when $b \to a$. The final shape solves the problem of reflections entirely, and is the form of a cosine function. However, in this case, Eq. (3) does not have an analytical solution, and therefore a numerical approach must be employed to calculate the value of $n(\theta)$.

This cloaking behavior is only exhibited if the rays or electromagnetic waves are confined to the surfaces under consideration. Two techniques can be employed to achieve this confinement. The first is to fill a thin, curved waveguide [21] with the index distribution, and the second is to utilize surface wave propagation. Surface wave supporting structures, with a variable refractive index, can be achieved with metasurfaces [22] or dielectric slabs (varying thickness or permittivity).

The first quantification is performed using waveguide structures. Figure 2 shows the simulations which demonstrate the performance of all three of the aforementioned surface cloaks. Figures 2(a)–2(c) illustrate the propagation of a plane wave incident from the left in a homogeneous dielectric filled waveguide of thickness $\lambda_m/10$, where λ_m is the wavelength in the medium for the hemispherical (a), conical (b), and cosine (c) waveguides. The radius of the curved part of the guide a is $4\lambda_m$. It is clear that the plane wave fronts are severely distorted by the curvature in all cases. Figures 2(d)–2(f) are simulations of the same three waveguide structures, when the dielectric filling the guide is replaced with the appropriate index for the curvature in the waveguide to be undetectable in the limit of geometrical optics. The refractive index distributions are shown in the insets. The values of refractive index shown are all normalized to have a lower boundary of unity, but they are valid for normalization to any positive minimum value, provided the whole distribution is scaled by the same value. This is equivalent to the flat space having a homogeneous refractive index which is nonunity, and equal to the scaling factor. All three cases, (d) the antifish eye cloak, (e) the conical cloak, and (f) the cosine cloak, can be seen to correct the phase difference, and reconstruct the plane wave fronts, although they suffer from varying degrees of shadowing due to reflections in the transition between the flat plane and the curved shape. As mentioned before, this is most severe in the hemispherical geometry, and it is only totally removed for the cosine geometry, which maintains the amplitude of the wave, effectively rendering the curvature in the waveguide completely invisible. Although a plane wave was selected for this demonstration, the cloak would also perform perfectly for any other form of excitation, such as a point source or a narrow beam.

In order for these cloaks to be utilized for a practical application, a surface wave implementation is investigated

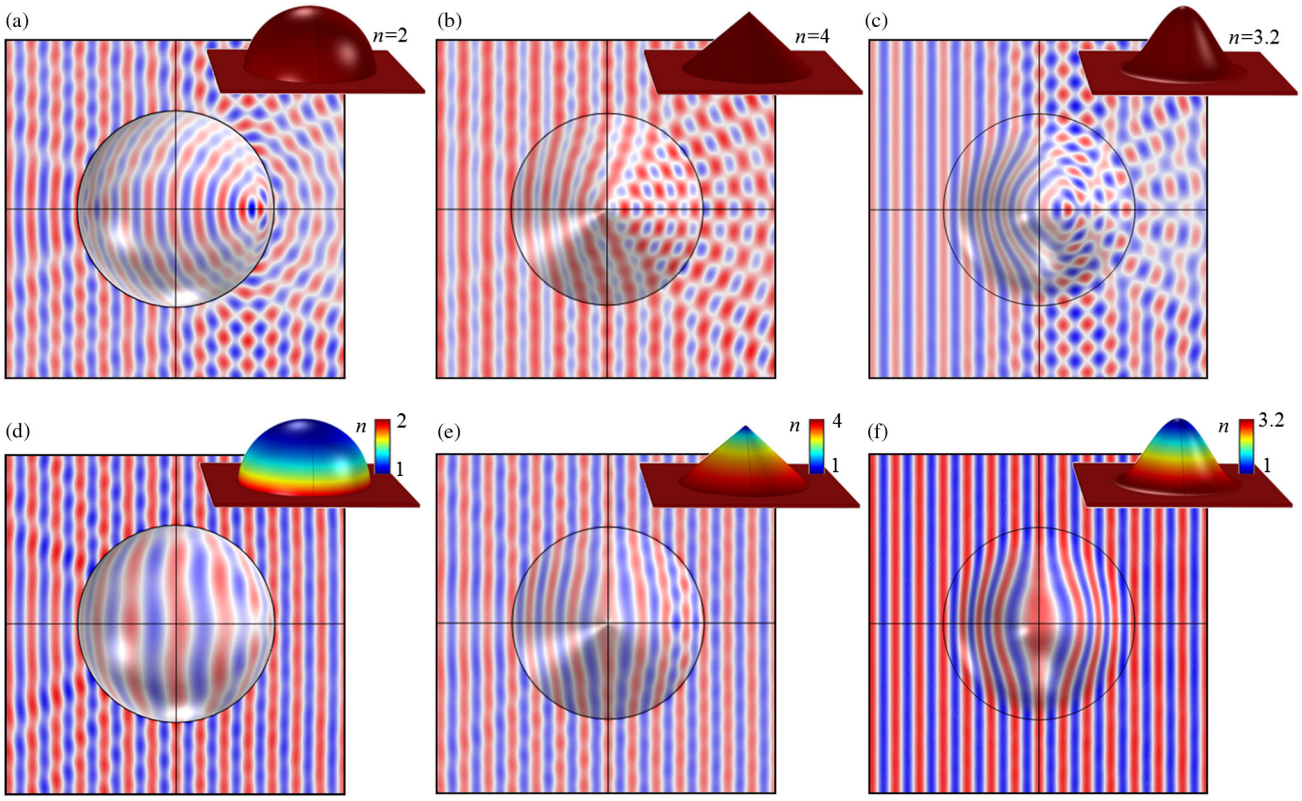

FIG. 2 (color online). Simulations of the wave propagation in waveguides with curved geometries, where the incident wave is a plane wave propagating from left to right. The insets illustrate the waveguide structure under investigation, with the refractive index n, of the medium filling the guide indicated. (a)–(c) Hemispherical, cone-shaped, and cosine-shaped waveguides filled with homogeneous material. (d)–(f) Hemispherical, cone-shaped, and cosine-shaped waveguides filled with the appropriate graded refractive index medium for them to become invisible to the incident plane wave.

using a graded dielectric slab above a ground plane. Any other surface wave implementation, such as metasurfaces [22] could be employed; however, a graded dielectric implementation is simple to fabricate with curved geometries. To achieve the appropriate propagation characteristics, it is necessary to alter the permittivity of the materials accordingly, for a given slab thickness, so that the effective refractive index achieves the required value. Figure 3 illustrates the required transformation of the dielectric constant of a 4.5 mm slab over a ground plane to achieve the equivalent refractive index at 10 GHz. The insets show the mode shape of the $|E_z|$ field component, which shows the confinement to the surface for a homogeneous slab with dielectric constants ε_r of 2, 7, 11, and 15, which were calculated using an eigenmode solver. The black line denotes the interface between the air and dielectric boundary, that are above and below, respectively, and the metallic ground plane is underneath the dielectric. The confinement is an important consideration for cloaking applications, to ensure minimal radiation from the surface when curved surfaces are employed. The relationship shown in Fig. 3 was used to calculate the required

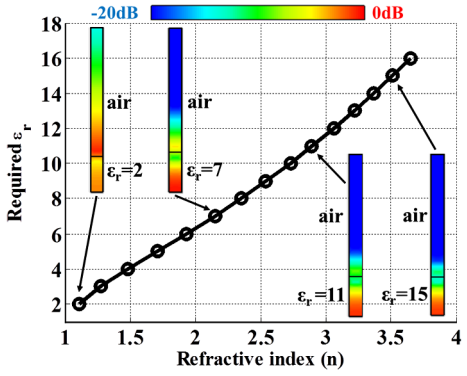

FIG. 3 (color online). Illustration of the required ε_r of a 4.5 mm slab against the obtained refractive index at 10 GHz. The insets are the $|E_z|$ field component and illustrate the confinement of the modes to the slab with $\varepsilon_r = 2$, 7, 11, and 15.

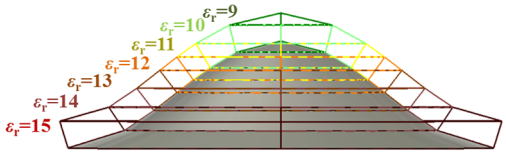

FIG. 4 (color online). Radial cross section of the discretized cloak design with seven distinct dielectric layers above a cosine shaped ground plane.

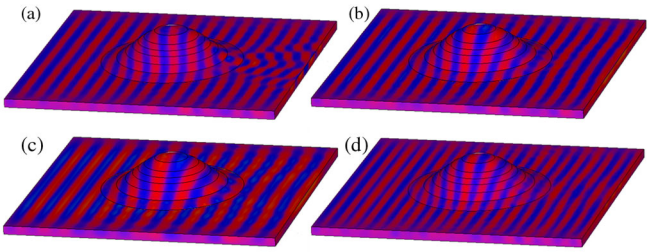

FIG. 5 (color online). Normal component of the electric field at the upper surface of the dielectric slab covering the metal cosine-shaped surface, where the excitation is a plane surface wave incident from the left. In (a) the slab is homogenous, and in (b)–(d) the slab consists of a seven layer cloaking structure. For (a) and (b) the simulations are performed at the 10 GHz design frequency, while (c) is at 8 GHz, and (d) at 12 GHz, demonstrating the frequency scanning performance.

permittivity profile to cloak a cosine surface with a maximum height b equal to half the radius, $a/2$. This cloak shape has a requirement of permittivity range of the order 1:1.7. The permittivities were chosen to range from 9–15 so that the upper end of Fig. 3 can be used where the confinement of the field to the surface is high. In order to evaluate the practical performance of this technique, a discretization process was performed on the continuous distribution to give a very simple seven- layered structure. Both the surface and the dielectric slab have linear boundaries, and the slab has a constant thickness perpendicular to the surface of the metallic ground plane, as illustrated in Fig. 4.

Figure 5 shows the perpendicular component of the electric field at the surface of the dielectric slab, which is positioned above the metallic, cosine-shaped ground plane. Figure 5(a) illustrates the perturbation to the plane surface wave when a homogenous slab is used. Figure 5(b) has the seven layer cloak covering the bump in the ground plane, and it can be seen that the plane wave incident on the left is reconstructed on the right (see Supplemental Material for the animated field propagation [23]). This crude discretization of the required profile demonstrates the robustness of this cloak design, and suggests that small deviations arising during any manufacturing process would not seriously influence the performance. Figures 5(c) and 5(d) show the frequency scanning performance for 8 and 12 GHz, respectively. Although the surface wave implementation was designed to operate at 10 GHz, this study demonstrates a bandwidth of operation at which the performance is shown to be accurate in the reconstruction of the plane wave fronts.

In conclusion, we have demonstrated the first practical proposal of an electromagnetic cloak applicable for surface waves. A robust method for designing surface wave cloaks that are rotationally symmetric, omnidirectional, and isotropic, without the requirement of superluminal propagation, is presented. This method can cloak objects that are electrically very large, yet the cloaks themselves are only a fraction of a wavelength in thickness. First, waveguide geometries are utilized to show the accurate performance of three different cloak designs. However, since only the cosine shape does not produce a discontinuity between the surface and the bump, this does not produce reflections. The latter cloak was then transformed into a surface wave implementation, after calculating the equivalent refractive index for the surface mode in dielectric slabs over a metallic ground plane. The performance is demonstrated to reconstruct the plane waves to a good accuracy, even for a coarse discretization of the index distribution, and for a range of frequencies, demonstrating the robustness of this technique. The presented results can be applied in the design of antennas and devices which rely upon surface waves that find practical applications in both microwave and THz regimes.

This work was funded by the Engineering and Physical Sciences Research Council (EPSRC), UK under a Programme Grant (EP/I034548/1) "The Quest for Ultimate Electromagnetics using Spatial Transformations (QUEST)."

*Corresponding author.
y.hao@qmul.ac.uk

[1] J. B. Pendry, D. Schurig, and D. R. Smith, Science **312**, 1780 (2006).
[2] U. Leonhardt, Science **312**, 1777 (2006).
[3] C. Argyropoulos, E. Kallos, and Y. Hao, Appl. Phys. A **103**, 715 (2011).
[4] D. Schurig, J. J. Mock, B. J. Justice, S. A. Cummer, J. B. Pendry, A. F. Starr, and D. R. Smith, Science **314**, 977 (2006).
[5] U. Leonhardt and T. Tyc, Science **323**, 110 (2009).
[6] P. A. Huidobro, M. L. Nesterov, L. Martin-Moreno, and F. J. Garcia-Vidal, Nano Lett. **10**, 1985 (2010).
[7] P. A. Huidobro, M. L. Nesterov, L. Martin-Moreno, and F. J. Garcia-Vidal, New J. Phys. **13**, 033011 (2011).
[8] M. Kadic, S. Guenneau, and S. Enoch, Opt. Express **18**, 12 027 (2010).
[9] M. Kadic, G. Dupont, S. Guenneau, and S. Enoch, J. Mod. Opt. **58**, 994 (2011).
[10] R. Yang and Y. Hao, Opt. Express **20**, 9341 (2012).
[11] B. Baumeier, T. A. Leskova, and A. A. Maradudin, Phys. Rev. Lett. **103**, 246803 (2009).
[12] J. Elser and V. A. Podolskiy, Phys. Rev. Lett. **100**, 066402 (2008).
[13] R. Quarfoth and D. Sievenpiper, *IEEE Antennas and Propagation Society International Symposium, Chicago* (IEEE, Bellingham, WA, 2012).
[14] M. Farhat, S. Enoch, S. Guenneau, and A. B. Movchan, Phys. Rev. Lett. **101**, 134501 (2008).
[15] M. Farhat, S. Guenneau, and S. Enoch, Phys. Rev. Lett. **103**, 024301 (2009).
[16] X. Shen, T. J. Cui, D. Martin-Cano, and F. J. Garcial-Vidal, Proc. Natl. Acad. Sci. U.S.A. **110**, 40 (2012).
[17] C. Pfeiffer and A. Grbic, IEEE Trans. Antennas Propag. **58**, 3055 (2010).

[18] O. Quevedo-Teruel, Prog. Electromagn. Res. **140**, 169 (2013).
[19] U. Leonhardt and T. G. Philbin, *Geometry and Light: The Science of Invisibility* (Dover, New York, 2010).
[20] M. Sarbort and T. Tyc, J. Opt. **14**, 075705 (2012).
[21] C. H. Walter, IRE Trans. Antennas Propag. **8**, 508 (1960).
[22] S. Maci, G. Minatti, M. Casaletti, and M. Bosiljevac, IEEE Antennas Wireless Propagat. Lett. **10**, 1499 (2011).
[23] See Supplemental Material at http://link.aps.org/supplemental/10.1103/PhysRevLett.111.213901 for animated field propagation of Figs. 5(a) and 5(b).